

1 Revised manuscript accepted for publication in Journal of Chromatography A, 2019,
2 10.1016/j.chroma.2019.460548.

3 **Salt and solvent effects in the microscale chromatographic** 4 **separation of heparan sulfate disaccharides**

5
6 Gábor Tóth^{a,b}, Károly Vékey^a, László Drahos^{a,1}, Viola Horváth^{b,c,1}, Lilla Turiák^{a,1*}

7

8 ^aMS Proteomics Research Group, Research Centre for Natural Sciences, Hungarian Academy
9 of Sciences, Magyar tudósok körútja 2., H-1117 Budapest, Hungary

10 ^bDepartment of Inorganic and Analytical Chemistry, Budapest University of Technology and
11 Economics, Szent Gellért tér 4., H-1111 Budapest, Hungary

12 ^cMTA-BME Computation Driven Chemistry Research Group, Szent Gellért tér 4., H-1111
13 Budapest, Hungary

14

15 ***Corresponding author**

16 Lilla Turiák
17 Research Centre for Natural Sciences, Hungarian Academy of Sciences,
18 Magyar tudósok körútja 2., H-1117, Budapest, Hungary
19 Email: turiak.lilla@ttk.mta.hu
20 Tel: +36 1 382 6516

21

22

23 **Author Contributions**

24 The manuscript was written through the contributions of all authors. All authors have given
25 approval to the final version of the manuscript.

26 ¹Contributed equally

27

28 **Conflict of interest**

29 The authors declare no conflict of interest.

30

31 **Abstract**

32 The analysis of heparan sulfate disaccharides poses a real challenge both from chromatographic
33 and mass spectrometric point of view. This necessitates the constant improvement of their
34 analytical methodology. In the present study, the chromatographic effects of solvent
35 composition, salt concentration, and salt type were systematically investigated in isocratic
36 HILIC-WAX separations of heparan sulfate disaccharides. The combined use of 75%
37 acetonitrile with ammonium formate had overall benefits regarding intensity, detection limits,
38 and peak shape for all salt concentrations investigated. Results obtained with the isocratic
39 measurements suggested the potential use of a salt gradient method in order to maximize
40 separation efficiency. A 3-step gradient from 14 mM to 65 mM ammonium formate
41 concentration proved to be ideal for separation and quantitation. The LOD of the resulting
42 method was 0.8-1.5 fmol for the individual disaccharides and the LOQ was between 2.5-5 fmol.
43 Outstanding linearity could be observed up to 2 pmol. This novel combination provided
44 sufficient sensitivity for disaccharide analysis, which was demonstrated by the analysis of
45 heparan sulfate samples from porcine and bovine origin.

46

47 **Keywords:** glycosaminoglycan; heparan sulfate; capillary liquid chromatography;
48 HILIC-WAX; salt gradient

49

50 **1. Introduction**

51 Glycosaminoglycans (GAGs) are long linear polysaccharides consisting of repeating
52 disaccharide units that comprise an amino sugar (N-acetylglucosamine or
53 N-acetylgalactosamine) and a hexuronic acid (HexA; glucuronic acid or iduronic acid) or
54 galactose and are sulfated along the chain which results in highly polar nature. The saccharide
55 units can be sulfated at various positions and epimerization may also occur along the chain.
56 They are localized in the extracellular matrix and on cell surfaces and are involved in numerous
57 biological functions, including organogenesis, cell adhesion, signaling, inflammation, and
58 tumorigenesis [1-3]. GAG chains may interact with different effector proteins (e.g. cytokines
59 and chemokines) and this interaction depends on sulfation motifs within the chain [4, 5].

60 Heparan sulfate (HS) is the class of GAGs carrying the largest diversity. It consists of HexA
61 and N-acetylglucosamine (GlcNAc) disaccharide units. Following the synthesis of the sugar
62 chain, epimerization of glucuronic acid to iduronic acid occurs in certain regions, and finally,
63 sulfation is carried out by sulfotransferases [6].

64 Due to their large size (up to 70 kDa), the investigation of intact HS chains is practically
65 impossible by instrumental analytical tools. The structural characterization of the average
66 sulfation pattern is usually performed after enzymatic hydrolysis of the polymeric chain into
67 the constituent disaccharide units [7]. Bacterial polysaccharide lyase enzymes degrade the
68 chains into $\Delta^{4,5}$ -unsaturated disaccharides with varying degrees of sulfation. The characteristics
69 of the resulting HS disaccharides are summarized in Table 1. Determining the ratio of these
70 different structures is important in understanding the mechanisms underlying several diseases.

71 Because of the above-mentioned facts, even the structural characterization of GAG
72 disaccharides poses several challenges [8]. Various chromatographic methods have been
73 reported to analyze $\Delta^{4,5}$ -unsaturated and sulfated HS disaccharides. These include
74 derivatization (for retention or detection) followed by reversed-phase chromatography [9-11],
75 reversed-phase ion-pairing chromatography (RPIP) [12-14], size exclusion chromatography
76 (SEC) [15-17], graphitized carbon [18, 19], amide-HILIC [20, 21], or HILIC-WAX [22, 23]
77 chromatography. Most of these separation methods can be on-line coupled to mass
78 spectrometry (MS) thus detailed structural information of GAGs can be acquired [24, 25]. The
79 main disadvantage of the above-mentioned methods is their relatively high detection limits,
80 most have LODs in the picomole, some in the high femtomole range [17, 22]. An excellent

81 review was written recently, by Solakyildirim, summarizing the recent advances of
82 glycosaminoglycan analysis [26].

83 We have recently reported an isocratic nanoflow HPLC-MS method [23] using self-packed
84 columns which allowed quantification of as few as 10 fmol HS disaccharides from four out of
85 the six investigated compounds. Sensitivity was an order of magnitude better than that of
86 previously reported methods. A mixed-mode resin combining hydrophilic interaction (HILIC)
87 and weak anion exchange (WAX) retention mechanisms was chosen as packing material, as it
88 enables separation of polar solutes based on charge, size, and polarity [22]. When an ion-
89 exchange column is operated under HILIC elution conditions, electric repulsion hydrophilic
90 interaction chromatography (ERLIC) is created [27], which is an efficient technique in the
91 separation of differently polarized components [28].

92 Building on our previously reported method [23], several further steps were considered in order
93 to maximize the performance of HS quantitation from limited sample amounts. Lower limits
94 were desirable especially for the non-sulfated D0A0 and the triply sulfated D2S6 disaccharides
95 which showed relatively high quantitation limits (20 fmol and 50 fmol, respectively).
96 To achieve this goal, it was necessary to increase the sensitivity of the individual disaccharides
97 and to obtain better peak shapes. Moreover, in order to increase throughput, a fast
98 chromatographic method with a more robust coupling (normal ESI source) was intended. In our
99 earlier work the pH, acetonitrile content and ammonium formate concentration were optimized
100 independently after one another, and the developed isocratic method was applied for the sample
101 preparation development and characterization of tissue microarrays. We have concluded that
102 acetonitrile gradients could not be applied due to the loss in sensitivity for the late eluting
103 doubly and triply sulfated disaccharides.

104 Since the above-mentioned parameters were observed to be interdependent, a detailed
105 investigation on the individual and cross-effects of acetonitrile content and salt concentration
106 showed great promise. Thus, we decided to map the individual and interaction effects through
107 a 3-factor experimental design operating with ammonium acetate and ammonium formate salts.

108 Although frequently used in ion (exchange) chromatography, salt gradients are almost entirely
109 neglected in HILIC-based chromatography, mainly because of the lack of theoretical
110 understanding of the retention mechanisms which still need theoretical and experimental
111 elucidation [29-31]. Using salt gradients in reversed-phase chromatography is also uncommon,
112 even for pH-gradient there are only a few reported examples [32, 33]. However, it was recently

113 proven that salt gradients can provide different selectivity, this way supplementing traditional
114 solvent gradients [34, 35].

115 Our aim was to pursue a detailed examination of the salt and solvent effects in the
116 chromatography of HS disaccharides to further improve throughput, quantitation limits, and
117 repeatability. As opposed to its rare previous utilization, we designed a method building on salt
118 gradients for HS disaccharide separation. The developed method proved to be applicable for
119 determining the sulfation pattern of HS chains from biological origin.

120 **2. Materials and Methods**

121 **2.1. Chemicals and reagents**

122 The $\Delta^{4,5}$ -unsaturated heparan sulfate disaccharide standards (listed in Table 1, 'HS
123 disaccharides' hereinafter) and heparan sulfate from porcine intestinal mucosa (HSPIM) were
124 purchased from Iduron (Cheshire, UK). LC-MS grade water and acetonitrile, crystalline
125 ammonium formate and ammonium acetate, formic acid and acetic acid, and heparan sulfate
126 from bovine kidney (HSBK) were purchased from Sigma-Aldrich (Budapest, Hungary).

127 **2.2. Column packing**

128 A GlycanPac™ AXH-1 1.9 μm analytical HPLC column (2.1x100mm, Thermo Fisher
129 Scientific, Waltham, MA USA) was unpacked and repacked into capillaries. For this purpose,
130 250 μm i.d. capillaries were cut and fritted as previously reported [36]. Briefly, capillaries were
131 dipped in a solution containing potassium silicate (Kasil® 1624, Kasil 1) and formamide in the
132 ratio of 3:1:1. The capillaries were then placed in an oven at 80 °C for 4 hours. After the fully
133 porous frit was produced, it was trimmed to 0.5 cm to reduce dead volume.

134 The packing itself was based on a method published recently [23] as follows. The capillary was
135 placed in a pressure injection cell and was washed with 1 mL methanol. A 1 mg/mL suspension
136 was prepared from the GlycanPac™ AXH-1 resin in 75% acetonitrile - 25% water. The slurry
137 was continuously vortexed using a magnetic stir bar and the column was packed using nitrogen
138 at 2000 psi. After reaching the desired 13 cm length, the pressure was carefully released
139 overnight. Finally, a 60-minute-long UPLC compression procedure at 8000 psi was applied to
140 maximize the axial homogeneity of the chromatographic bed.

141 **2.3. Liquid chromatography-mass spectrometry**

142 For microscale chromatography, a 'hybrid' system was assembled. The in-house packed
143 capillary column was mounted on a Waters® nanoAcquity UPLC system (Waters, Milford,
144 MA, USA) coupled to a high-resolution Waters® QTOF Premier™ Mass Spectrometer
145 (Waters, Milford, MA, USA) via normal electrospray ionization source.

146 **2.3.1. MS parameters**

147 The mass spectrometry parameters were optimized for the highest sensitivity avoiding
148 undesirable fragmentation in the ion source by directly infusing Leucine Enkephalin, D0A0,
149 and D2S6 standards and further optimized via HPLC measurements. The capillary voltage was
150 set to 2.4 kV, sampling cone to 20 eV, extraction cone to 4 V, the ion guide to 1.5. The source
151 temperature was 80 °C, the desolvation temperature was 100 °C, the cone gas was 25 L/h and
152 the desolvation gas 300 L/h. The investigated compounds were measured as singly-charged

153 anions (deprotonated molecules, $[M-H]^-$). Multiply charged ions or adduct forms complicating
154 the analysis were not observed.

155 **2.3.2. UHPLC parameters**

156 For the investigation of the chromatographic behavior, we injected a mixture of the HS
157 standards: 1 pmol of D0A0, D0S0, D2A6; 0.5 pmol of the D2A0 and D0A6 standards
158 (positional isomers, thus resulting in a total of 1 pmol D2A0/D0A6 content); 2.5 pmol of D2S0
159 and D0S6 (positional isomers, thus resulting in a total of 5 pmol D2S0/D0S6 content) and 5
160 pmol of the D2S6 standard. The injection of this mixture resulted in similar peak heights.

161 The flow rate was selected to be 8 $\mu\text{L}/\text{min}$ based on the stability of the signal investigated in a
162 flow injection study (details not shown).

163 The column temperature was adjusted using an AgileSleeve capillary heater with MonoSleeve
164 column heater controller (Analytical Sales and Services Inc, Flanders, NJ USA). The
165 temperature was optimized and thermostating at 45°C was found optimal for the
166 chromatographic performance (details not shown).

167

168 **2.4. Screening of salt effects with ammonium formate**

169 **2.4.1. Mobile phase preparation**

170 Mobile phase solvents were prepared by dissolving ammonium formate in water, then formic
171 acid was added in an acid-to-salt molar ratio of 0.13 to adjust the pH to a previously optimized
172 value of 4.4 [23], and finally, acetonitrile was added.

173 **2.4.2. Solvent composition and salt content in isocratic methods**

174 The effects were investigated by isocratic measurements at the respective salt concentration and
175 solvent composition. The eluents were prepared with 75%, 50% and 25% acetonitrile content,
176 and in each case 5 mM, 10 mM, 15 mM, 20 mM, 25 mM, 30 mM, 35 mM, 45 mM, 55 mM,
177 and 65 mM ammonium formate concentrations were adjusted.

178 As a further optimization step, isocratic methods using 80%, 75%, 70%, 65% and 60%
179 acetonitrile content were also tested, in order to justify that the formerly established 75%
180 acetonitrile content provides the optimal conditions. The salt concentration for these runs was
181 set to 45 mM.

182 **2.5. Screening of salt effects with ammonium acetate**

183 After optimizing the acid-to-salt molar ratio to reach the necessary pH of 4.4, and minimize
184 ion-suppression, the same experimental design was performed as in the case of ammonium
185 formate.

186 **2.6. Salt gradient method**

187 Based on the results of the isocratic screening, we designed a salt gradient method using the
188 following parameters. Eluent A: 10 mM ammonium formate in 75:25 v/v ACN:water (pH 4.4);
189 Eluent B: 65 mM ammonium formate in 75:25 v/v ACN:water (pH 4.4).

190 The flow rate was 8 μ L/min and the gradient program was the following: after 0.5 minutes
191 isocratic flow at 6% B, then the eluent ratio changed in 3 minutes to 70% B, then in 1 minute
192 to 90% B, finally to 100% B in 4 minutes. 100% B solvent composition was held for 1.5 minutes
193 and was followed by a 9-minute-long equilibration at the initial composition.

194

195 **2.7. Enzymatic digestion of heparan sulfate**

196 300 ng heparan sulfate from HSPIM/HSBK was dissolved in 45 μ L aqueous digestion solution
197 (12.5 mM ammonium bicarbonate, 2.5 mM Ca(OH)₂ containing 2.5 mU of Heparan Lyase I,
198 2.5 mU of Heparan Lyase II, and 1.25 mU of Heparan Lyase III). Following 24 hours of
199 incubation at 37 °C, another cycle of enzymes (2.5 mU of Heparan Lyase I, 2.5 mU of Heparan
200 Lyase II, and 1.25 mU of Heparan Lyase III) in 5 μ L volume was added and the mixture was
201 incubated at 37 °C for 24 more hours. The reaction was quenched by heating the sample to
202 80 °C for 5 minutes. The samples were dried down and re-dissolved in 50 μ L ‘gradient starting
203 solvent’ from which 2 μ L was injected containing 12 ng HS portions.

204

205 **2.8. Data evaluation and interpretation**

206 Chromatographic parameters, like resolution, peak area, and intensity values were calculated
207 with the QuanLynx add-in of Waters MassLynx 4.1 software. Then, the data were imported to
208 OriginPro 8 to visualize in a contour plot using default settings of the program.

209

210 3. Results and discussion

211 3.1. Solvent and salt effects

212 Previous findings suggest that both salt concentration and solvent composition may have crucial
213 effects on the separation efficiency of HS disaccharides in HILIC-WAX chromatography. In
214 these studies, we used an acetonitrile-water solvent system with ammonium formate salt. We
215 had previously tested a methanol-water solvent system as well, but it produced worse results.
216 The combined effects of ammonium formate concentration and acetonitrile-water solvent ratio
217 were mapped using a 3x10 factorial design. Three different acetonitrile contents were studied,
218 75%, 50%, and 25%. Initial studies have shown that acetonitrile content higher than 75%
219 resulted in wide and shallow peaks, so we did not exceed this range for detailed investigations
220 in the current study. Ammonium formate content was studied in the 5-65 mM range using 10
221 steps. This way we mapped the whole range that can be conveniently used for HPLC coupled
222 to MS. It is important to note that even at high salt concentration we have observed no
223 contamination of the ion source and the MS signals were stable over several weeks of analysis.

224 The key objectives in studying the effect of salt concentration and solvent composition were
225 the proper separation of early eluting components, improving the resolution of monosulfated
226 (D0S0-D2A0/D0A6) and disulfated (D2A6-D2S0/D0S6) peak pairs, eluting highly sulfated
227 components in a relatively short time, and providing good sensitivity of analysis for all
228 components. Note, that D2A0/D0A6 and D2S0/D0S6 disaccharides are positional isomers
229 having practically identical hydrophilicity and charge, respectively, thus their separation is not
230 feasible in this setup. The effect of salt concentration on the separation of the HS disaccharides
231 is demonstrated in Fig. 1 (at 75% acetonitrile content), while that of solvent composition is
232 shown in Fig. 2 (at 25 mM ammonium formate concentration). These effects are discussed in
233 detail below in terms of retention factor, selectivity, resolution, sensitivity (peak area), and S/N
234 ratio (intensity) parameters.

235 The first criterion is, that all the target compounds should be eluted from the column in a
236 reasonable time, presuming appropriate retention and selectivity. Plotting retention factors as a
237 function of salt concentration and solvent composition (Fig. 3), the changes were remarkable.
238 Increasing salt concentration resulted in a fast decrease in the retention factors for all the
239 components at all solvent compositions. Relatively low (10 mM) ammonium formate
240 concentration (Fig. 1A) gave unsatisfactory results: retention factors were too high, thus not all
241 components eluted in the 25-minute elution window. Increasing salt concentration to 25 mM
242 resulted in a remarkable improvement (Fig. 1B). Using even higher (45 mM) salt concentration

243 (Fig. 1C) further decreased the retention factors, but this also resulted in co-elution of several
244 components, mainly monosulfated (peaks 2, 3) and disulfated (peaks 4, 5) HS disaccharides
245 which are closest to each other in polarity.

246 Increasing water content also changed the retention factors, although to a lower degree, and
247 unequally for various components. Retention factors of non-sulfated and monosulfated
248 disaccharides (peaks 1, 2, 3) showed a minor decrease with elevated water content, while those
249 for doubly and triply sulfated disaccharides (peaks 4, 5, 6) increased, and co-elution of
250 monosulfated (peaks 2, 3) and doubly sulfated components (peaks 4, 5) occurred (Fig. 2 and
251 Fig. 3).

252 In highly aqueous solvents ion-exchange mechanism dominates, thus ions are distinguished
253 primarily by the number of their charges, therefore co-elution of similarly charged
254 disaccharides occur.

255 Second, we considered the resolution (R) of monosulfated and doubly sulfated peak pairs an
256 important indicator for chromatographic separation. The contour plots in Fig. 4 show the change
257 in resolution of the monosulfated (Fig. 4A) and the disulfated (Fig. 4B) peak pairs. As both the
258 peak width and retention time decreased with increased salt concentration (as seen in Fig. 1) it
259 was important to find a balance between these two to maximize resolution. The highest
260 resolution of monosulfated components can be achieved by using relatively low (5-15 mM)
261 ammonium formate concentration, while the resolution of disulfated HS disaccharides
262 increased practically monotonously with increasing salt concentration at 75% acetonitrile
263 content, and elaborately at other solvent compositions. This suggested that using a salt gradient
264 may be optimal for the analysis of sulfated disaccharides.

265 A further important factor to consider is the overall sensitivity in ESI mass spectrometry.
266 In fact, in most biological applications this is of crucial importance. Although proper
267 quantitation is typically based on peak area, for optimal sensitivity, peak intensity (related to
268 S/N ratio, being best for narrow peaks) may be even more important. The average peak areas,
269 peak heights, and signal-to-noise ratios as a function of salt concentration and solvent
270 composition are shown in the contour plots in Fig. 4C, 4D, and 4E, respectively. These show
271 that sensitivity decreases fast with decreasing acetonitrile content with respect to both peak
272 areas and peak intensities, due to lower ionization efficiency and increasing peak width.
273 Increasing salt concentration (going from bottom to top on the contour plots) influenced peak
274 areas only slightly, but (due to sharper peaks) intensities and the S/N ratio increased
275 substantially. These imply that ion suppression or deterioration of ion source conditions do not
276 happen even at elevated salt concentrations.

277 The results discussed above show that optimal solvent composition was found at the high edge
278 of the investigated range, so we have performed further experiments (at 45 mM ammonium
279 formate content) to map the range of 65% - 80% acetonitrile ratio in detail. It was found
280 (analogously to that reported earlier [23]) that the best results were obtained at 75% acetonitrile
281 content. Using 65-70% acetonitrile content resulted in a decreased resolution. Increasing
282 acetonitrile content to 80% resulted in approximately 5-times increase in peak widths, resulting
283 in a major loss (3-5-fold) of peak intensities (Fig. A-1). As it is seen in Fig. A-2, S/N ratios had
284 a maximum at 70% ACN, the peak areas had maximum at 75% and 80%, but peak height had
285 a large maximum at 75%. For this reason, we decided not to study solvent compositions over
286 75% in more detail.

287 Besides ammonium formate, the other commonly used buffer salt in HILIC-based separations
288 (especially when on-line coupled to mass spectrometry) is ammonium acetate. We repeated the
289 study discussed above using ammonium acetate. This study did not yield any further
290 information: salt concentration and solvent composition had the same effects as obtained with
291 ammonium formate. However, chromatographic peak shapes were more asymmetric, and mass
292 spectrometry sensitivity was also worse. The data are shown in details in Appendix B.

293 **3.2. Discussion of retention mechanism**

294 The GlycanPac AXH-1 column is a HILIC-WAX mixed-mode resin, the chemistry of which is
295 unknown for the public. The HILIC functional group is used to retain very polar compounds,
296 and the WAX property separates based on charge. Discussing the possible interactions
297 governing retention is rather difficult due to the unknown stationary phase chemistry and the
298 mixed-mode operation. The solvation of the analytes and their dissociation states are strongly
299 influenced by the acetonitrile ratio in the mobile phase [37]; and the fact that besides the
300 effective pH [38, 39], the ionic strength may also have an influence [29], further complicating
301 the picture. Instead of the pure HILIC and WAX operation conditions, their resultant determines
302 the retention. Besides, the amino group in the HS disaccharides may be protonated under
303 operating conditions, thus electric repulsion hydrophilic interaction chromatography (ERLIC)
304 mechanism might also play a role [27]. This means that under HILIC conditions, the positively
305 charged WAX functional groups repel the molecules that bear a protonated amino group.
306 Bearing all of these in mind, we would like to propose an explanation for the interactions
307 governing the retention of HS disaccharides on a HILIC-WAX column.

308 25% acetonitrile (thus high water) content in the mobile phase provides ideal circumstances for
309 ion exchange, while under such high water content the HILIC effect is inoperative. In WAX,

310 the interaction of the analytes with both the stationary and the mobile phase is based on ionic
311 effects, and therefore separation is mainly due to charge differences. Under such conditions, it
312 is not possible to separate the mono- and the disulfated HS disaccharides, respectively. This
313 mode of action is illustrated in Fig. 3, where at 25% acetonitrile content these components
314 coelute (Fig. 3C).

315 Increasing acetonitrile content up to 50%, WAX interactions are weakened, and HILIC effects
316 start to modify chromatography. The retention of non-sulfated and monosulfated components
317 are hardly affected, while retention decrease of doubly and triply sulfated components becomes
318 significant (Fig. 3B). Note, that the interactions affected by acetonitrile content may cause
319 further changes [37], but their detailed investigation and discussion is out of the scope of the
320 present paper.

321 Using 75% acetonitrile content, chromatographic effects are fairly complicated. Under such
322 conditions, the HILIC functionality becomes dominant, while the WAX functionality may
323 switch from ionic interactions to electric repulsion hydrophilic interaction chromatography
324 (ERLIC). Separation is determined by the combination of the two. This is shown by the
325 increased retention of non-sulfated and monosulfated disaccharides compared to lower
326 acetonitrile content (Fig. 3A vs Fig. 3B). On the other hand, the retention of di- and trisulfated
327 disaccharides decreases significantly due to the switch of WAX related strong retention to
328 HILIC and ERLIC. The large selectivity increase between N-sulfated and N-acetylated
329 disaccharides of the same charge can be explained as follows. N-sulfation decreases the electron
330 density of the N-atom, the protonation is less likely, this way the effect of ERLIC is smaller;
331 this is corroborated by the larger retention times of N-sulfated components (D0S0 and
332 D2S0/D0S6) compared to the respective N-acetylated compounds (D2A0/D0A6 and D2A6).

333 In mixed-mode separations, the orientation of the various molecules may also play a crucial
334 role [40], therefore even small structural differences result in increased separation. At 75%
335 ACN content, planar coordination of the molecules is likely, as the proximity of O-sulfate
336 groups to the amino group has no effect, while modification of the N-acetyl group has a large
337 effect on retention. In contrast, at 50% and 25%, acetonitrile content the column operates
338 mainly as an anion exchanger, and the coordination of the sulfate groups to the stationary phase
339 has no effect on the strength of retention.

340 In summary, the degree of significance of HILIC, WAX and ERLIC mechanisms on the
341 retention behavior depends on both the sulfation degree (i.e. charge state) of the various

342 compounds and the experimental conditions. Multiply charged disaccharides exhibit strong
343 ionic interactions with the stationary phase and their retention is governed predominantly by
344 the ion-exchange process in the whole experimental space (mostly WAX, partly ERLIC).
345 HILIC, on the other hand, provides a substantial contribution to the retention of disaccharides
346 with a lower number of sulfate groups present, especially at high acetonitrile content and at low
347 salt concentration. Finally, when the acetonitrile content is increased above 75%, HILIC-type
348 interactions with the stationary phase become very strong, and the various disaccharides do not
349 elute from the column in a reasonable time (see Fig. A-1 and A-2).

350 **3.3. Salt gradient separation of HS disaccharides**

351 Results of the isocratic screening discussed above show that best separation characteristics
352 (in terms of sensitivity, peak shape, and resolution) were obtained using 75% ACN – 25% H₂O
353 solvent composition with ammonium formate buffering salt. However, separation of all
354 components in reasonable run time and at high sensitivity could not be achieved simultaneously
355 for all components using a constant salt concentration. Applying a generally used solvent
356 gradient would have no significant benefits, as this would result either in bad elution
357 characteristics or poor sensitivity (as seen in Fig. 3 and 4). Another alternative, rarely used in
358 HILIC-based separations, is applying a salt gradient. The concept was to start the run at
359 relatively low ammonium formate concentration (10-15 mM) so that the non-sulfated and
360 monosulfated components were baseline-separated, then apply a moderately fast salt gradient
361 to decrease the retention time and to increase intensity/sensitivity of the highly sulfated
362 components. Note that this concept resolved the most important limitations of the previously
363 reported HILIC studies, i.e. low sensitivity, badly resolved, and often irreproducible peaks for
364 highly sulfated HS disaccharides. Detailed information on the development of the 3-step
365 gradient is shown in Appendix C.

366 We designed a salt gradient method which used a 3-step gradient starting from 14 mM to 65 mM
367 ammonium formate concentration. This way we have obtained a chromatogram (Fig. 5) with
368 close to ideal peak shapes (FWHM of the last peak was practically the same as that of the first
369 peak), good resolution, selectivity, and sensitivity. Note that salt concentration had a crucial
370 effect on the retention and peak shape, but in contrary to usual mass spectrometry experience,
371 it caused no additional ion suppression and gave no problems even in the long run (over several
372 weeks). Resolution for all peak pairs was over 1.5, except that of the D2A6-D2S0/D0S6 peak
373 pair, which was around 1.3. We considered this separation acceptable, especially as the two
374 components have different molecular mass; separating them by mass spectrometry is trivial.

375 For the D0A0 and the D2S0/D0S6 components, the limit of quantitation (LOQ, defined
376 according to the FDA Bioanalytical Method Validation guidelines [41]) was determined at 5
377 fmol, while for the D0S0, D0A6/D2A0, D2A6, and D2S6 components the LOQs were below
378 2.5 fmol. The limit of detection (LOD, estimated as 3-times S/N) was approximately 1.5 fmol
379 for D0A0 and D2S0/D0S6, and below 1 fmol for the other components. These values show that
380 our method is 100 times more sensitive than one of the recent papers on heparan sulfate analysis
381 [22], and approximately 2-10 better than obtained before [23] using the same instrument in
382 isocratic mode. Improved sensitivity may be attributed to gradient focusing and lower noise
383 observed.

384 The linearity of the method was characterized in a wide range from 2.5 fmol to 2 pmol, each
385 concentration was measured in triplicate. The R^2 values covering the whole range were all
386 above 0.99, except in the case of D0A0, where it was 0.98. Calibration curves are shown in the
387 Supplementary Information plotted both in linear and logarithmic mode (Fig. A-2).

388 The repeatability of the method was analyzed in 5 consecutive runs (intra-day repeatability) on
389 3 different days of the week (inter-day repeatability) using a 1 pmol HS disaccharide standard
390 mixture. Intra-day repeatability (relative standard deviation of peak areas) was 3% on average,
391 while inter-day repeatability was 5% (Table A-1). The retention time stability was 0.32 %
392 intra-day, and 0.73% inter-day (RSD values). Long-term robustness of the system was
393 outstanding; around 3 months of problem-free operation was observed when working with these
394 high salt-content methods. Furthermore, no carry-over was experienced, even after injecting as
395 much as 10 pmol samples.

396 **3.4. Analysis of heparan sulfate samples**

397 Performance of the developed method has been tested in the case of two different HS samples,
398 which have been studied before [20, 42]. The samples, derived from porcine intestinal mucosa
399 (HSPIM) and bovine kidney (HSBK), were enzymatically degraded with bacterial lyase
400 enzymes into unsaturated HS disaccharides. Four replicates of digested samples were injected
401 and separated using the developed salt gradient μ HPLC-MS method. The sulfation pattern of
402 heparan sulfate was demonstrated by the relative abundance of the HS disaccharides (Fig. 6).
403 The non-sulfated D0A0, the disulfated D2S0/D0S6, and the triply sulfated D2S6 were the
404 dominant disaccharides in both samples, while the disulfated D2A6 disaccharide was present
405 only in a negligible amount. The monosulfated disaccharides, D0S0 and D0A6/D2A0, were
406 present in moderate amounts in both samples. The ratio of the multiply sulfated components

407 was lower in the bovine than in the porcine sample, thus the degree of sulfation was much lower
408 in HSBK than in HSPIM. This can be numerically described by the average number of sulfate
409 groups on disaccharides, which is 0.96 for HSBK and 1.92 for HSPIM. These results agree well
410 with previously reported data [20, 42]. The relative standard deviation of peak areas for all
411 components in both samples remained under 20%, except for the D2S6 in HSBK (21.79%),
412 present in relatively low amount. These RSD values are considered acceptable contemplating
413 the variability of the biological samples, the difficult sample preparation steps, and the low
414 amounts of the measured disaccharides.

415

416 **4. Conclusions**

417 The HPLC-MS analysis of heparan sulfate disaccharides poses a challenge from both
418 chromatography and mass spectrometry sides, due to their diverse polarity and unfavorable
419 ionization characteristics. In this paper, we performed a detailed isocratic screening of salt and
420 solvent effects through a factorial design. We found that the acetonitrile-water ratio of the
421 solvent highly influenced both the elution characteristics and ionization efficiency. Altering the
422 salt concentration improved elution characteristics, but did not cause problems on the mass
423 spectrometry side of the analysis.

424 Based on the above-mentioned results, we developed a salt gradient operating with self-packed
425 HILIC-WAX μ HPLC columns coupled to ESI mass spectrometry working in negative ion
426 mode. Using the salt gradient improved sensitivity and repeatability could be achieved,
427 compared to previous methods using the same resin [22, 23]. It was possible to separate and
428 quantify the unsaturated HS disaccharides down to a few femtomoles, using a relatively short,
429 20-minute-long gradient. Sulfation patterns of heparan sulfates determined using the present
430 method gave analogous results to those determined using other techniques.

431 The developed salt gradient method on mixed-mode HILIC-WAX resin offers several
432 advantages as compared to previously published methods. First, the method is shorter than any
433 other method reported (20 minutes instead of 30-60 minutes) [15-18, 20, 26]. Second, it
434 provides utmost sensitivity with LOD below 1 fmol for all HS disaccharides (min. 100 fmol
435 with other resins, and 10-50 fmol with HILIC-WAX was possible before). Furthermore, it
436 facilitates proper investigation of non-sulfated and triply sulfated components in a single run.

437

438 **Acknowledgments**

439 Supported by the ÚNKP-18-3-II-BME-230 New National Excellence Program of the Ministry
440 of Human Capacities, Viola Horváth being a supervisor.

441 Lilla Turiák and Károly Vékey acknowledge the support of the National Research Development
442 and Innovation Office (OTKA PD 121187, and OTKA 119459) and Lilla Turiák is grateful for
443 the support of the János Bolyai Research Scholarship of the Hungarian Academy of Sciences.

444

445

446 **Appendices**

447 **Appendix A - Supplementary figures and tables**

448 **Figure A-1.** Effects of solvent ratios surrounding 75% acetonitrile. A: 70% ACN; B: 75%
449 ACN; C: 80% ACN content. The ammonium formate concentration was set to 45 mM, which
450 resulted in sharp peaks but moderate resolution using 75% ACN content.

451 **Figure A-2.** Effects of solvent ratios surrounding 75% acetonitrile on average peak area (red),
452 average peak height (blue), and average signal-to-noise ratio (black). The ammonium formate
453 concentration was set to 45 mM at all points.

454 **Figure A-3.** The linearity of the method, calibration curves for the individual HS disaccharide
455 standards: D0A0 (A), D0A6/D2A0 (B), D0S0 (C), D2A6 (D), D2S0/D0S6 (E), and D2S6 (F).

456 **Table A-1.** Intra-Day and Inter-Day repeatability of analysis characterized by the relative
457 standard deviation of peak areas and retention times for HS disaccharides.

458 **Appendix B - Ammonium acetate isocratic screening**

459 **Appendix C - Development of the 3-step gradient**

460

461 **List of tables**

462 **Table 1.** Structure, nomenclature, and m/z values of the HS disaccharides investigated. Note,
463 that D2A0/D0A6 and D2S0/D0S6 are positional isomers and are not distinguished in the
464 present study.

465

466 **List of figures**

467 **Figure 1.** Effect of different salt concentrations using 75 % acetonitrile – 25% water solvent
468 composition. Sums of extracted ion chromatograms (EICs) are shown in the diagram for A:
469 10 mM (not sufficient elution); B: 25 mM (sufficient resolution); and C: 45 mM (insufficient
470 retention and resolution) ammonium formate salt concentrations.

471 **Figure 2.** Sums of EICs indicating the changes caused by different solvent compositions using
472 25 mM ammonium formate concentration. A: 75% ACN; B: 50% ACN; C: 25% ACN.

473 **Figure 3.** Retention factor (k) values of individual disaccharides as a function of ammonium
474 formate salt concentration. Results are shown for three solvent compositions separately (A:
475 75% ACN; B: 50% ACN; C: 25% ACN content). Missing points mean that the respective
476 component did not elute within the 25-minute elution window.

477 **Figure 4.** Resolution values of D0S0 - D2A0/D0A6 (A) and D2A6 - D2S0/D0S6 peak
478 pairs (B), average peak areas (C), average peak intensities (D), and average signal-to-noise
479 ratios (E) of all the HS disaccharides plotted on a contour plot as a function of salt concentration
480 and acetonitrile content of the solvents. Color codes with the corresponding values are
481 incorporated in the figure for each plot.

482 **Figure 5.** Extracted ion chromatograms of HS disaccharides obtained by separating 1 pmol of
483 each compound using the developed salt gradient method.

484 **Figure 6.** The sulfation patterns of heparan sulfate from porcine intestinal mucosa (HSPIM)
485 and bovine kidney (HSBK). The sulfation pattern of the respective compound is characterized
486 by the relative abundance of the HS disaccharides present following bacterial lyase digestion.

487

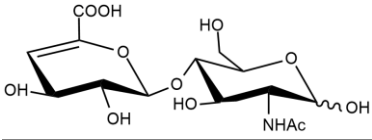
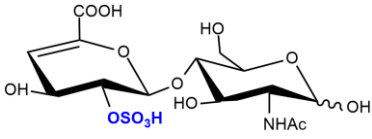
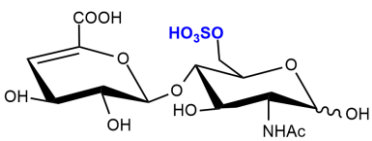
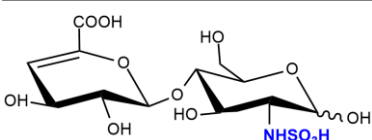
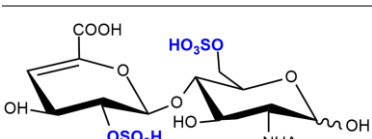
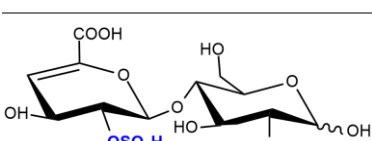
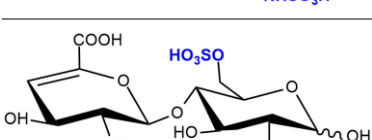
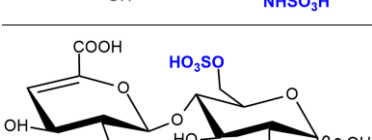
488 **References**

- 489 1. Handel, T.M., et al., *Regulation of protein function by glycosaminoglycans--as exemplified by*
490 *chemokines*. Annu Rev Biochem, 2005. **74**: p. 385-410.
- 491 2. Karthikeyan, S. and S. Barbara, *Tumor-dependent Effects of Proteoglycans and Various*
492 *Glycosaminoglycan Synthesizing Enzymes and Sulfotransferases on Patients' Outcome*.
493 *Current Cancer Drug Targets*, 2019. **19**(3): p. 210-221.
- 494 3. Lin, H.-Y., et al., *The relationships between urinary glycosaminoglycan levels and phenotypes*
495 *of mucopolysaccharidoses*. Molecular Genetics & Genomic Medicine, 2018. **6**(6): p. 982-992.
- 496 4. Gibbs, R.V. *Cytokines and Glycosaminoglycans (GAGS)*. 2003. Boston, MA: Springer US.
- 497 5. Kjellen, L. and U. Lindahl, *Specificity of glycosaminoglycan-protein interactions*. Current
498 *Opinion in Structural Biology*, 2018. **50**: p. 101-108.
- 499 6. Mulhaupt, H.A.B. and J.R. Couchman, *Heparan sulfate biosynthesis: methods for*
500 *investigation of the heparanosome*. The journal of histochemistry and cytochemistry : official
501 *journal of the Histochemistry Society*, 2012. **60**(12): p. 908-915.
- 502 7. Lawrence, R., et al., *Disaccharide structure code for the easy representation of constituent*
503 *oligosaccharides from glycosaminoglycans*. Nat Methods, 2008. **5**(4): p. 291-292.
- 504 8. Zaia, J., *Principles of mass spectrometry of glycosaminoglycans*. Journal of
505 *Biomacromolecular Mass Spectrometry*, 2005. **1**(1): p. 3-36.
- 506 9. Galeotti, F. and N. Volpi, *Online Reverse Phase-High-Performance Liquid Chromatography-*
507 *Fluorescence Detection-Electrospray Ionization-Mass Spectrometry Separation and*
508 *Characterization of Heparan Sulfate, Heparin, and Low-Molecular Weight-Heparin*
509 *Disaccharides Derivatized with 2-Aminoacridone*. Anal. Chem, 2011. **83**(17): p. 6770-6777.
- 510 10. Volpi, N., et al., *Analysis of glycosaminoglycan-derived, precolumn, 2-aminoacridone-labeled*
511 *disaccharides with LC-fluorescence and LC-MS detection*. Nat. Protoc, 2014. **9**(3): p. 541-558.
- 512 11. Pan, Y., et al., *Glycosaminoglycans from fish swim bladder: isolation, structural*
513 *characterization and bioactive potential*. Glycoconj J, 2017.
- 514 12. Yang, B., et al., *Ultra-performance ion-pairing liquid chromatography with on-line*
515 *electrospray ion trap mass spectrometry for heparin disaccharide analysis*. Anal. Biochem,
516 2011. **415**(1): p. 59-66.
- 517 13. Wang, B., et al., *Characterization of currently marketed heparin products: Analysis of heparin*
518 *digests by RPIP-UHPLC-QTOF-MS*. J. Pharmaceut. Biomed, 2012. **67-68**: p. 42-50.
- 519 14. Zhang, Z.Q., et al., *Quantification of Heparan Sulfate Disaccharides Using Ion-Pairing*
520 *Reversed-Phase Microflow High-Performance Liquid Chromatography with Electrospray*
521 *Ionization Trap Mass Spectrometry*. Anal. Chem, 2009. **81**(11): p. 4349-4355.
- 522 15. Hitchcock, A.M., C.E. Costello, and J. Zaia, *Glycoform quantification of chondroitin/dermatan*
523 *sulfate using a liquid chromatography-tandem mass spectrometry platform*. Biochemistry,
524 2006. **45**(7): p. 2350-2361.
- 525 16. Shi, X.F. and J. Zaia, *Organ-specific Heparan Sulfate Structural Phenotypes*. J. Biol. Chem,
526 2009. **284**(18): p. 11806-11814.
- 527 17. Shao, C., et al., *Mass spectral profiling of glycosaminoglycans from histological tissue*
528 *surfaces*. Anal. Chem, 2013. **85**(22): p. 10984-10991.
- 529 18. Barroso, B., M. Didraga, and R. Bischoff, *Analysis of proteoglycans derived sulphated*
530 *disaccharides by liquid chromatography/mass spectrometry*. J. Chromatogr. A, 2005. **1080**(1):
531 p. 43-48.
- 532 19. Karlsson, N.G., et al., *Use of graphitised carbon negative ion LC-MS to analyse enzymatically*
533 *digested glycosaminoglycans*. J. Chromatogr. B, 2005. **824**(1-2): p. 139-147.
- 534 20. Gill, V.L., et al., *Disaccharide Analysis of Glycosaminoglycans Using Hydrophilic Interaction*
535 *Chromatography and Mass Spectrometry*. Analytical Chemistry, 2013. **85**(2): p. 1138-1145.
- 536 21. Takegawa, Y., et al., *Simultaneous Analysis of Heparan Sulfate, Chondroitin/Dermatan*
537 *Sulfates, and Hyaluronan Disaccharides by Glycoblotting-Assisted Sample Preparation*

- 538 Followed by Single-Step Zwitter-Ionic-Hydrophilic Interaction Chromatography. *Anal. Chem*,
539 2011. **83**(24): p. 9443-9449.
- 540 22. Chen, J.H., et al., *Heparan sulfate: Resilience factor and therapeutic target for cocaine abuse*.
541 *Sci Rep*, 2017. **7**.
- 542 23. Turiak, L., et al., *Sensitive method for glycosaminoglycan analysis of tissue sections*. *J*
543 *Chromatogr A*, 2018. **1544**: p. 41-48.
- 544 24. Ucakturk, E., et al., *Changes in composition and sulfation patterns of glycoaminoglycans in*
545 *renal cell carcinoma*. *Glycoconjugate J*, 2016. **33**(1): p. 103-112.
- 546 25. Bruinsma, I.B., et al., *Sulfation of heparan sulfate associated with amyloid-beta plaques in*
547 *patients with Alzheimer's disease*. *Acta Neuropathol*, 2010. **119**(2): p. 211-220.
- 548 26. Solakyildirim, K., *Recent advances in glycosaminoglycan analysis by various mass*
549 *spectrometry techniques*. *Analytical and Bioanalytical Chemistry*, 2019. **411**(17): p. 3731-
550 3741.
- 551 27. Alpert, A.J., *Electrostatic Repulsion Hydrophilic Interaction Chromatography for Isocratic*
552 *Separation of Charged Solutes and Selective Isolation of Phosphopeptides*. *Analytical*
553 *Chemistry*, 2008. **80**(1): p. 62-76.
- 554 28. Lorocho, S., et al., *Multidimensional electrostatic repulsion-hydrophilic interaction*
555 *chromatography (ERLIC) for quantitative analysis of the proteome and phosphoproteome in*
556 *clinical and biomedical research*. *Biochim Biophys Acta*, 2015. **1854**(5): p. 460-468.
- 557 29. Alpert, A.J., *Effect of salts on retention in hydrophilic interaction chromatography*. *J*
558 *Chromatogr A*, 2018. **1538**: p. 45-53.
- 559 30. Buszewski, B. and S. Noga, *Hydrophilic interaction liquid chromatography (HILIC)--a powerful*
560 *separation technique*. *Anal Bioanal Chem*, 2012. **402**(1): p. 231-247.
- 561 31. Naidong, W., *Bioanalytical liquid chromatography tandem mass spectrometry methods on*
562 *underivatized silica columns with aqueous/organic mobile phases*. *Journal of*
563 *Chromatography B*, 2003. **796**(2): p. 209-224.
- 564 32. Kaliszan, R., P. Wiczling, and M.J. Markuszewski, *pH Gradient Reversed-Phase HPLC*.
565 *Analytical Chemistry*, 2004. **76**(3): p. 749-760.
- 566 33. Vreeker, G.C.M. and M. Wuhrer, *Reversed-phase separation methods for glycan analysis*.
567 *Analytical and Bioanalytical Chemistry*, 2017. **409**(2): p. 359-378.
- 568 34. Mant, C.T., et al., *An improved approach to hydrophilic interaction chromatography of*
569 *peptides: Salt gradients in the presence of high isocratic acetonitrile concentrations*. *Journal*
570 *of Chromatography A*, 2013. **1277**: p. 15-25.
- 571 35. Mant, C.T. and R.S. Hodges, *Mixed-mode hydrophilic interaction/cation-exchange*
572 *chromatography: separation of complex mixtures of peptides of varying charge and*
573 *hydrophobicity*. *Journal of separation science*, 2008. **31**(9): p. 1573-1584.
- 574 36. Maiolica, A., D. Borsotti, and J. Rappsilber, *Self-made frits for nanoscale columns in*
575 *proteomics*. *Proteomics*, 2005. **5**(15): p. 3847-3850.
- 576 37. Xia, J. and P.J. Gilmer, *Organic modifiers in the anion-exchange chromatographic separation*
577 *of sialic acids*. *Journal of Chromatography A*, 1994. **676**(1): p. 203-208.
- 578 38. Espinosa, S., E. Bosch, and M. Rosés, *Retention of Ionizable Compounds on HPLC. 12. The*
579 *Properties of Liquid Chromatography Buffers in Acetonitrile-Water Mobile Phases That*
580 *Influence HPLC Retention*. *Analytical Chemistry*, 2002. **74**(15): p. 3809-3818.
- 581 39. Subirats, X., M. Rosés, and E. Bosch, *On the Effect of Organic Solvent Composition on the pH*
582 *of Buffered HPLC Mobile Phases and the pK_a of Analytes—A Review*. *Separation &*
583 *Purification Reviews*, 2007. **36**(3): p. 231-255.
- 584 40. Alpert, A.J., et al., *Peptide Orientation Affects Selectivity in Ion-Exchange Chromatography*.
585 *Analytical Chemistry*, 2010. **82**(12): p. 5253-5259.
- 586 41. Food And Drug Administration, U.S., *Bioanalytical Method Validation. Guidance for Industry*.
587 2018.
- 588 42. Shao, C., et al., *Mass Spectral Profiling of Glycosaminoglycans from Histological Tissue*
589 *Surfaces*. *Analytical Chemistry*, 2013. **85**(22): p. 10984-10991.

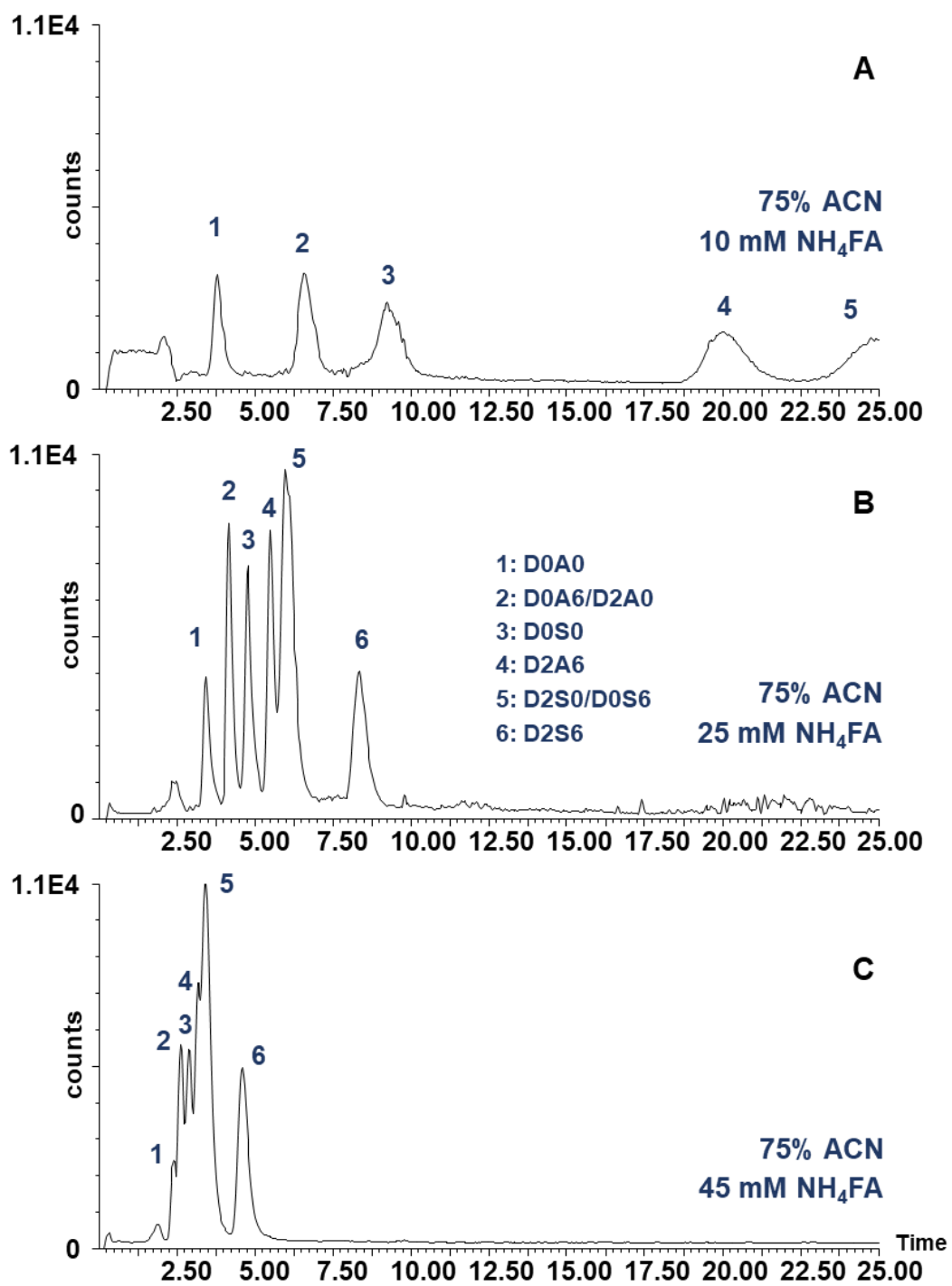
590 **Table 1.** Structure, nomenclature, and m/z values of the HS disaccharides investigated. Note,
 591 that D2A0/D0A6 and D2S0/D0S6 are positional isomers and are not distinguished in the
 592 present study.

593

Chemical structure	Traditional name	Lawrence code	m/z (-) mode
	ΔHexA-GlcNAc	D0A0	378.1
	ΔHexA2S-GlcNAc	D2A0	458.1
	ΔHexA-GlcNAc6S	D0A6	458.1
	ΔHex-GlcNS	D0S0	416.1
	ΔHexA2S-GlcNAc6S	D2A6	538.1
	ΔHexA2S-GlcNS	D2S0	496.1
	ΔHex-GlcNS6S	D0S6	496.1
	ΔHexA2S-GlcNS6S	D2S6	576.1

594

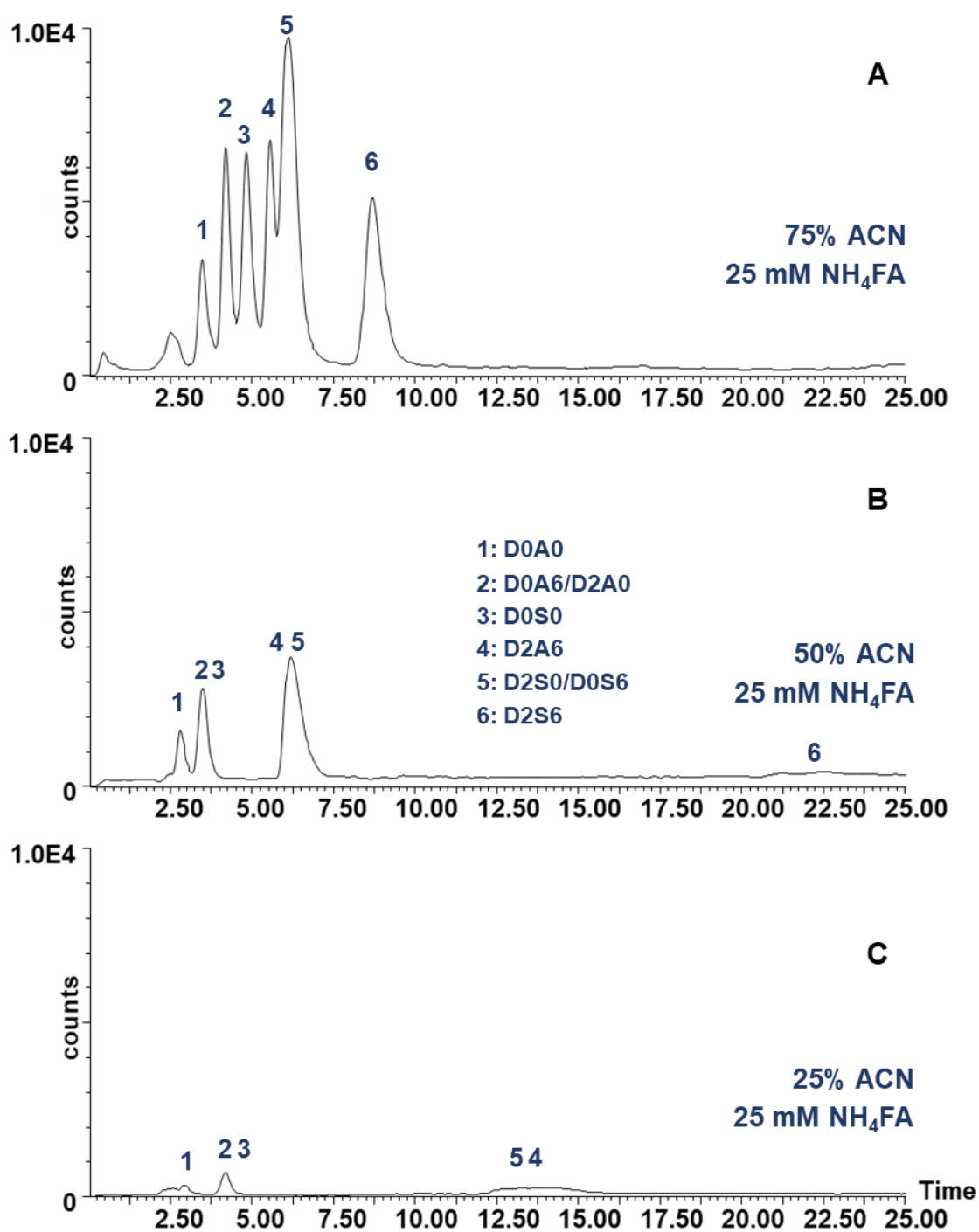
595



596

597 Fig. 1.

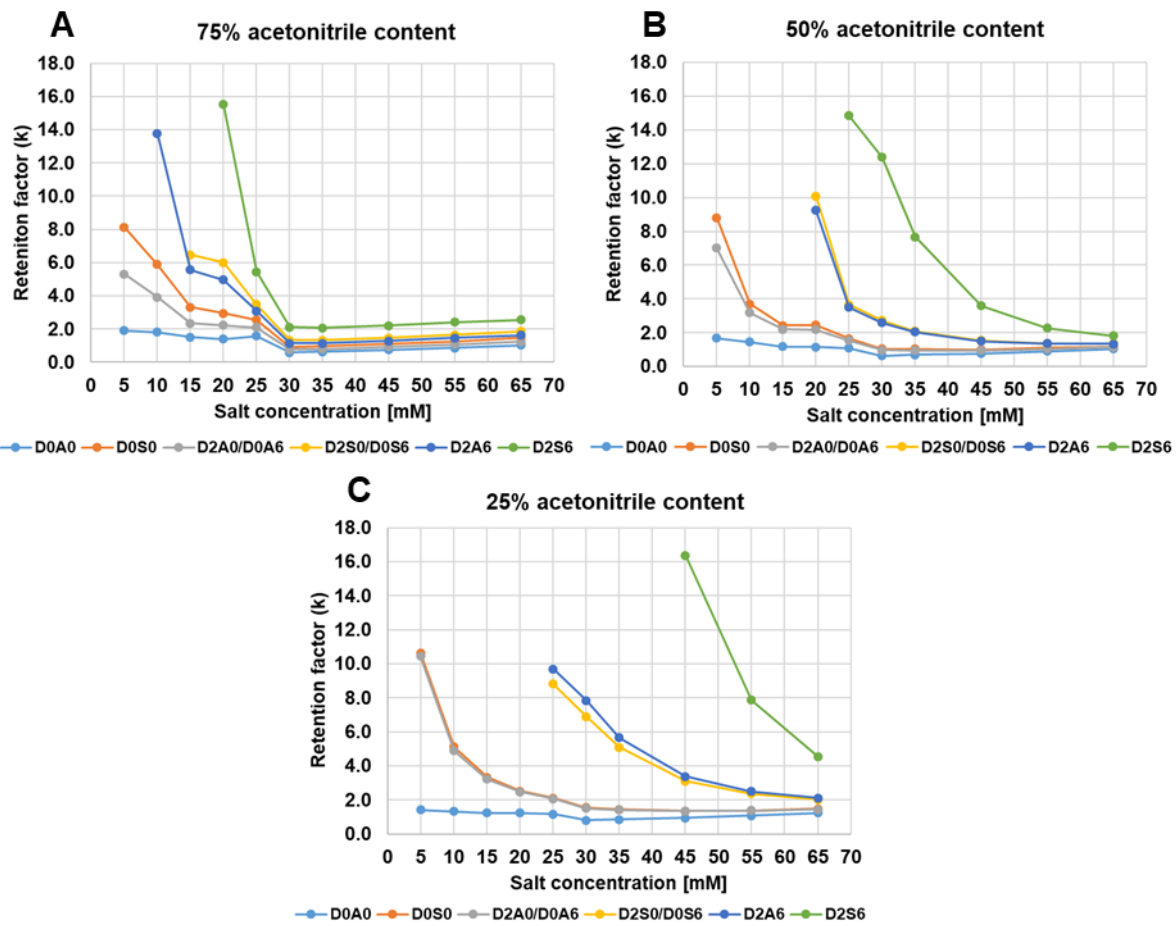
598



599

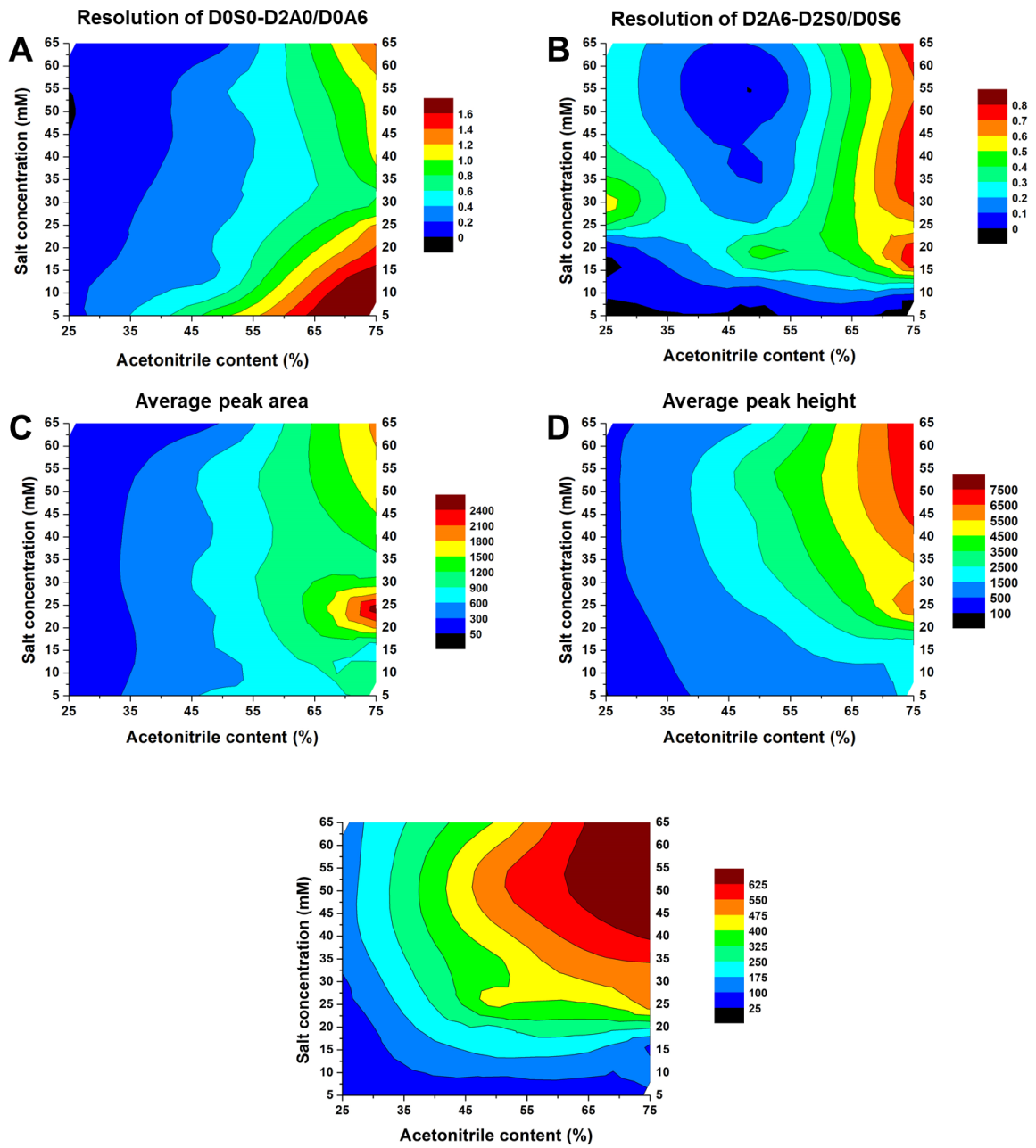
600 Fig. 2

601



602

603 Fig.3



604

605 **Fig.4**

606

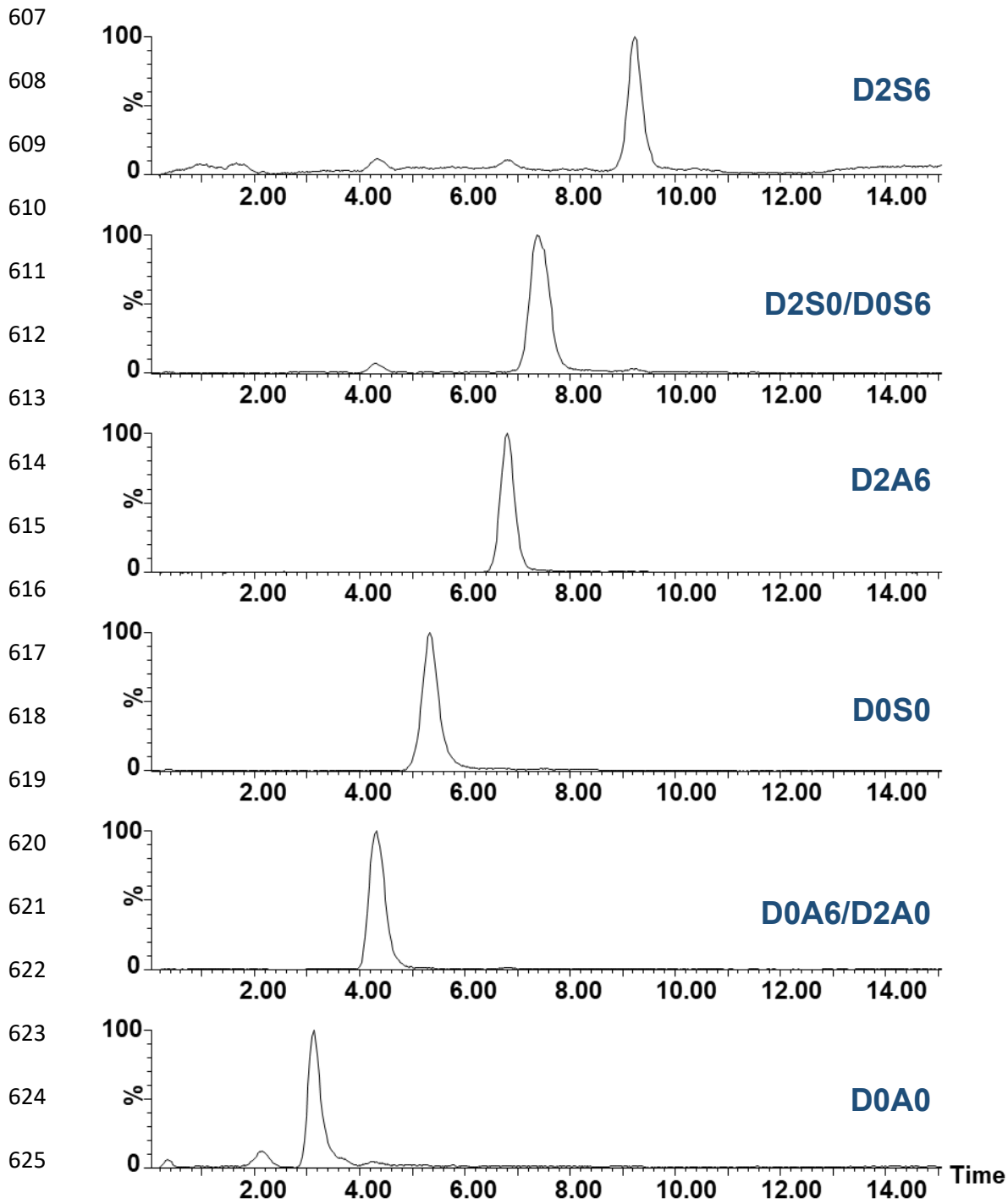
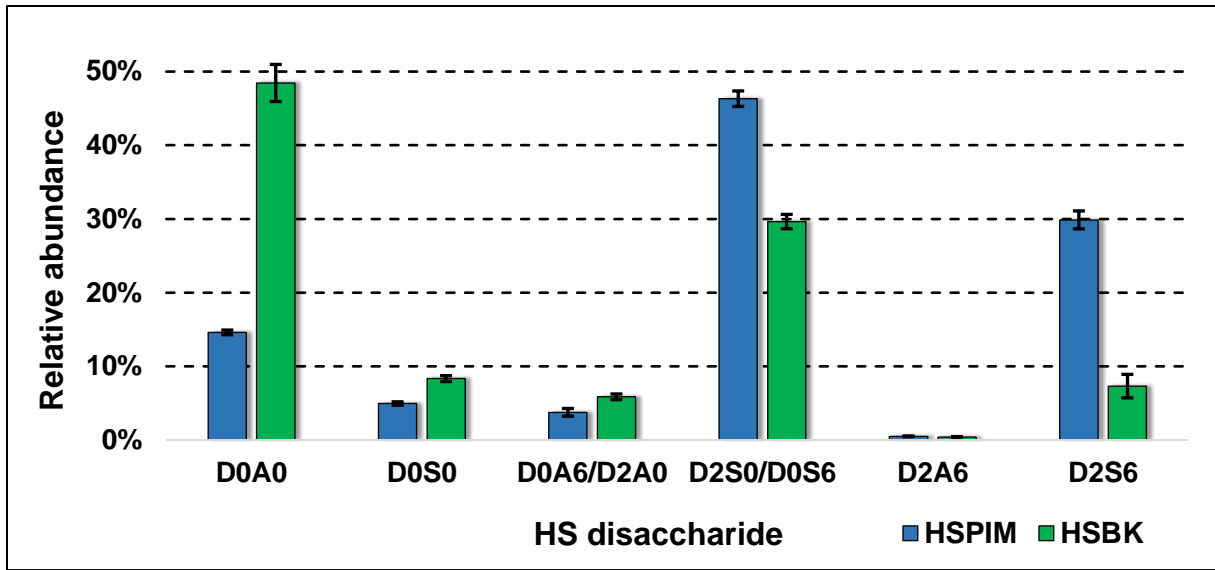


Fig.5



629

630 Fig.6